

Induced Formation of Primordial Low-Mass Stars

R. Salvaterra¹, A. Ferrara¹, R. Schneider^{2,3}

¹*SISSA/International School for Advanced Studies, Via Beirut 4, 34100 Trieste, Italy*

²*INAF/Osservatorio Astrofisico di Arcetri, L.go E. Fermi 5, 50125 Firenze, Italy*

³*“Enrico Fermi” Center, Via Panisperna 89/A, 00184 Roma, Italy*

24 February 2019

ABSTRACT

We show that the explosion of the first pair-unstable supernovae can trigger low-mass star formation via gravitational fragmentation of the supernova-driven gas shell. The necessary conditions for such instability are: (i) the mean density of the ambient medium is $14 \text{ cm}^{-3} < n_0 < 790 \text{ cm}^{-3}$; (ii) the explosion energy $E_{SN} > 3 \times 10^{52} \text{ erg}$ (i.e. core-collapse supernovae are not suitable triggers). The typical mass of the unstable fragments is $\sim 10^{5-6} M_{\odot}$; their density is in the range $8 \times 10^3 - 10^9 \text{ cm}^{-3}$. Fragments have a metallicity strictly lower than $10^{-2.6} Z_{\odot}$ and large values of the gravitational-to-pressure force ratio $f \gtrsim 400$. Based on these findings, we conclude that the second generation of stars produced by such self-propagating star formation is predominantly constituted by low-mass, long-living, extremely metal-poor (or even metal-free, if mixing is suppressed) stars. We discuss the implications of such results for Pop III star formation scenarios and for the recently discovered most iron-poor halo star HE0107-5240.

Key words: galaxies: formation - first stars - cosmology: theory

1 INTRODUCTION

As many recent numerical (Bromm, Coppi & Larson 1999, 2002; Abel, Bryan & Norman 2000) and semi-analytical (Schneider *et al.* 2002, Omukai & Inutsuka 2002, Omukai & Palla 2003) studies have shown, the first luminous objects, the so called Population III (Pop III) stars, are likely to be very massive. According to these studies, stars with a characteristic mass of 100-600 M_{\odot} originate in the primordial gas, whereas low mass objects should not have formed due to the lack of heavy elements. High mass stars are indeed required to account for the unexplained Near Infrared Background (Salvaterra & Ferrara 2003; Magliocchetti, Salvaterra & Ferrara 2003). Bromm *et al.* (2001) and Schneider *et al.* (2002) have shown that there exists a critical metallicity ($Z_{cr} = 10^{-5 \pm 1} Z_{\odot}$) setting the transition from a high-mass to a low-mass fragmentation mode of star formation. The exact value of Z_{cr} depends on the fraction of heavy elements that are depleted onto dust grains (Schneider *et al.* 2003). In this scenario, a gas cloud with a metallicity $Z \sim 10^{-5.1} Z_{\odot}$ can lead to the formation of low mass stars if $\sim 20\%$ of the heavy elements is in dust grains (Schneider *et al.* 2003). The recent discovery of the most iron-poor star ($[\text{Fe}/\text{H}] = -5.3 \pm 0.2$) ever seen in our Galaxy (Christlieb *et al.* 2002) could be an example of such low-mass metal poor stars originated from a gas with mean metallicity of $10^{-5.1} Z_{\odot}$ (Schneider *et al.* 2003; but see Umeda & Nomoto (2003), who have pointed out that this star could have in-

stead formed from a carbon-rich, iron-poor gas, with a corresponding mean metallicity of $10^{-2} Z_{\odot}$).

An alternative potentially viable mechanism to form low-mass, metal-poor stars does exist. Indeed, Nakamura & Umemura (2001, 2002, hereafter NU01 and NU02) have studied the collapse and fragmentation of filamentary primordial gas clouds using one- and two-dimensional hydrodynamical simulations coupled with the nonequilibrium processes of molecular hydrogen formation. They have shown that filaments with relatively low initial density ($n \lesssim \text{few} \times 10^4 \text{ cm}^{-3}$) tend to fragment into dense clumps before the central density reaches $10^8 - 10^9 \text{ cm}^{-3}$; the fragment mass is around 100 M_{\odot} . In contrast, if a filament has initially a larger density, fragmentation continues until the clumps become optically thick to H_2 lines, leading to a typical fragment mass of $\sim 1 M_{\odot}$. So the resulting IMF of first stars would be bimodal, with a low-mass peak around $\sim 1 - 2 M_{\odot}$ and a high-mass peak at a few hundred M_{\odot} . Mackey *et al.* (2003) have suggested that these low-mass peak stars could form in the gas shocked by the explosion of the first generation of very massive supernovae (SNe).

In this paper, we put this hypothesis on a more quantitative basis. We will show that the shell is gravitationally unstable only for large explosion energies and that gravitationally unstable clumps are likely to form long-living, low-mass, metal-poor stars, that could be detected through dedicated surveys as the Hamburg/ESO objective prism survey (Christlieb *et al.* 2001).

The paper is organized as follows. In Section 2 we calculate the SN-driven shell evolution and derive the conditions for gravitational instability. In Section 3 we examine the instability in the expanding shell for different explosion energies and interstellar medium (ISM) densities, whereas in Section 4 we calculated the properties of unstable fragments. In Section 5 we constrain the fragment metallicity; Section 6 discusses the consequences for Pop III star formation scenarios.

2 EVOLUTION OF THE SHELL

We study the evolution of a SN-driven shell in the interstellar medium using the thin shell approximation (Ostriker & McKee 1988; Madau, Ferrara & Rees 2001). The momentum and energy conservation yield the following relevant equations:

$$\frac{d}{dt}(V_{sh}\rho_0\dot{R}_{sh}) = 4\pi R_{sh}^2(P_b - P), \quad (1)$$

$$\frac{dE_b}{dt} = L - 4\pi R_{sh}^2 P_b \dot{R}_{sh} - V_{sh} \bar{n}_{H,b}^2 \Lambda(\bar{T}_b), \quad (2)$$

where the subscripts ‘*sh*’ and ‘*b*’ indicate shell and bubble quantities, respectively. Here, R_{sh} is the shell radius, $V_{sh} = (4\pi/3)R_{sh}^3$ is the volume enclosed by the shell; the overdots represent time derivatives. P and $\rho_0 = \mu m_H n_0$ are the pressure and the density of the ISM (n_0 is the gas number density and $\mu = 0.59$ is the mean molecular weight of a primordial ionized H/He mixture). The shell expansion is driven by the internal energy E_b of the hot bubble gas, whose pressure is $P_b = E_b/2\pi R_{sh}^3$ (for a gas with adiabatic index $\gamma = 5/3$). Finally, $\bar{n}_{H,b}^2 \Lambda(\bar{T}_b)$ is the cooling rate per unit volume of the hot bubble gas, whose average hydrogen density and temperature are $\bar{n}_{H,b}$ and \bar{T}_b , respectively. L is the luminosity corresponding to a total explosion energy E_{SN} . The right-hand side of eq. (1) represents the momentum gained by the shell from the SN-shocked wind, while the right-hand side of eq. (2) describes the mechanical energy input, the work done against the shell, and the energy losses due to radiation.

Neglecting the ambient gas pressure and cooling, the solution of the above equations is given by the analytic expression derived by Sedov (1959):

$$R_{sh} = 1.15 \left(\frac{E_{SN}}{\rho_0} \right)^{1/5} t^{2/5}, \quad (3)$$

where t is the time elapsed from the explosion. As cooling becomes important for the swept up gas, the shock is no longer driven by the heated gas and the evolution enters the momentum conserving phase, satisfying the familiar ‘Oort snowplow’ solution, $R_{sh} \propto t^{1/4}$.

2.1 Cooling time

The cooling time is given by

$$t_{cool} = \frac{3}{2} \frac{kT_b}{n_{ps}\Lambda(T_b)}, \quad (4)$$

where $n_{ps} = n_0(\gamma + 1)/(\gamma - 1)$ is the post-shock density for an adiabatic shock, and $\Lambda(T_b)$ is the cooling function for a

primordial gas. The evolution of the post-shock temperature T_b is given by (Madau, Ferrara, Rees 2001)

$$\frac{dT_b}{dt} = 3 \frac{T_b}{R_{sh}} \dot{R}_{sh} + \frac{T_b}{P_{sh}} \dot{P}_{sh} - \frac{23}{10} \frac{C_1}{C_2} \frac{kT_b^{9/2}}{R_{sh}^2 P_{sh}}. \quad (5)$$

where $C_1 = 16\pi\mu m_p \eta/25k$ and $C_2 = (125/39)\pi\mu m_p$ and $\eta = 6 \times 10^{-7}$ (c.g.s. units) is the classical Spitzer thermal conduction coefficient (we have assumed a Coulomb logarithm equal to 30). This relation closes the system of equations (1)-(2).

If the shell lives for sufficiently long time (i.e. $t_{cool} \ll t$), the gas cools down to a final temperature $T_f \sim 300$ K. This temperature is the minimum temperature provided by cooling from H₂ molecules forming under nonequilibrium conditions in the post-shock gas (Ferrara 1998).

2.2 Perturbations in the shell

The linear growth of perturbations in an expanding shell was derived by Elmegreen (1994). Expansion tends to suppress (stabilize) the growth of density perturbations owing to stretching, hence counteracting the self-gravity pull. The instantaneous maximum growth rate is

$$\omega = -\frac{3v_{sh}}{R_{sh}} + \left[\left(\frac{v_{sh}}{R_{sh}} \right)^2 + \left(\frac{\pi G \rho_0 R_{sh}}{3c_{s,sh}} \right)^2 \right]^{1/2}, \quad (6)$$

where $c_{s,sh} = (kT_f/\mu m_H)^{1/2}$ is the sound speed in the shell and v_{sh} is the velocity of the expanding shell. Instability occurs only if $\omega > 0$, or

$$\frac{v_{sh}}{R_{sh}} < \frac{1}{8^{1/2}} \frac{\pi G \rho_0 R_{sh}}{3c_{s,sh}} \propto \frac{t_{cross}}{t_{ff}^2}, \quad (7)$$

where $t_{cross} \sim R_{sh}/c_{s,sh}$ is the crossing time in the shell and t_{ff} is the free-fall time. Furthermore, if the fragment mass is close to (but slightly above) the Jeans mass, the $\omega > 0$ condition translates into $v_{sh}/R_{sh} < 1/t_{ff}$. So, large shell velocity-to-radius ratios inhibit the formation of gravitationally unstable fragments. These relations are derived under the assumption of supersonic motion, i.e. $v_{sh}(t) > c_{s,0}$, where $c_{s,0}$ is the sound speed in the ISM. If the shock decays into a pressure wave before the onset of the instability (i.e. before $\omega > 0$), no fragmentation will take place and the shell will be dispersed by random gas motions.

The most rapidly growing mode has wavelength

$$\lambda_f = \frac{6c_{s,sh}^2}{G\rho_0 R_{sh}} [1 + (1 - \xi^2)^{1/2}]^{-1}, \quad (8)$$

where the dimensionless parameter ξ is given by

$$\xi = \left(\frac{8^{1/2} v_{sh}}{R_{sh}} \right) \left(\frac{\pi G \rho_0 R_{sh}}{3c_{s,sh}} \right).$$

We will show later that the typical fragment size ($R_f = \lambda_f/2$) is greater than the thickness of the shell $\Delta R_{sh} = v_{sh} t_{cool}$; in this case it is likely that disk-like fragments form of mass

$$M_f = \pi \rho_{sh} \Delta R_{sh} R_f^2, \quad (9)$$

where ρ_{sh} is the mean density in the thin shell, given by the ratio between its mass M_{sh} (equal to the shell swept up mass) and its volume V_{sh}

$$\rho_{sh} = \frac{M_{sh}}{V_{sh}} = \frac{4}{3}\rho_0 \frac{R_{sh}}{\Delta R_{sh}}. \quad (10)$$

For subsequent purposes we define the ratio of gravitational-to-pressure force:

$$f = \frac{\pi G \rho_{sh} R_f^2}{2kT_f}. \quad (11)$$

3 INSTABILITY IN THE EXPANDING SHELL

We solve numerically Eq. (1)-(2) and Eq. (5) for different values of the unperturbed ISM density n_0 , and of the explosion energy, E_{SN} , following the time evolution of the shell radius (R_{sh}) and velocity (v_{sh}). The unperturbed medium is assumed to be metal free, and its temperature is taken to be equal to 10^4 K, as the medium has been probably ionized by the SN progenitor. At each time step we check the supersonic motion ($v_{sh} > c_{s,0}$) and instability ($\omega > 0$) conditions. If both conditions are satisfied we further check that the cooling time is shorter than the age of the shell, so that the temperature has decreased to $T_f \sim 300$ K. At this point we calculate the fragment density (Eq. 10), mass (Eq. 9), and the ratio f (Eq. 11).

We consider here SN energies in the range $10^{51} - 10^{53}$ erg, the lower limit being typical of Type II SN explosions and the upper limit corresponding to the energy released by the most massive pair-instability SN ($\text{SN}_{\gamma\gamma}$) explosions (Heger & Woosley 2002). We explore the range of ISM densities $n_0 = 10^{-2} - 10^4 \text{ cm}^{-3}$. Fig. 1 shows the time-evolution of the shell radius and velocity for $n_0 = 10^2 \text{ cm}^{-3}$ and three explosion energies. The bottom panel shows the corresponding evolution of the instability growth rate ω . Only the most energetic explosion ($E_{SN} = 10^{53}$ erg) induces shell instability and fragmentation.

Fig. 2 shows the region of the parameter space $E_{SN} - n_0$ where both the conditions $\omega > 0$ and $v_{sh} > c_{s,0}$ are verified and therefore the shell is gravitationally unstable. We find that this occurs only for explosion energies $E_{SN} \gtrsim 3 \times 10^{52}$ erg and densities $14 \lesssim n_0 \lesssim 790 \text{ cm}^{-3}$. The lower limit is dictated by the limited mass growth of the shell before the shock decays into a pressure wave; above the upper limit, the shell is decelerated by the large ISM pressure before becoming unstable.

We conclude that the first pair-instability SNe with energies larger than 3×10^{52} erg (corresponding to stellar masses $M_* > 190 M_\odot$) are able to trigger self-propagating star formation under a wide range of ambient conditions, whereas expanding shells created by less energetic ‘normal’ or subluminous (as those proposed by Shigeyama & Tsujimoto 1998) Type II SNe cannot fragment.

4 PROPERTIES OF THE FRAGMENTS

Let us now explore in more details the properties of the gravitationally unstable fragments. As it is clear from Eqs. (8)-(9) the fragment mass is a function of the explosion energy (through R_{sh} and v_{sh}), of the initial density of the

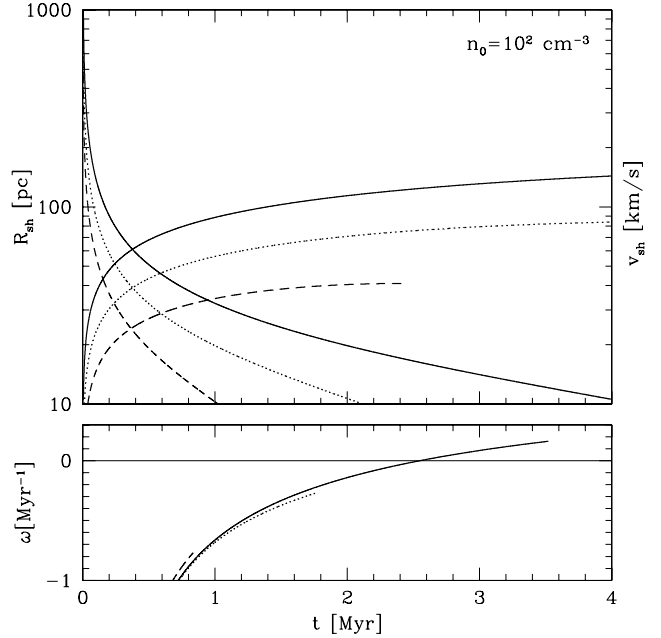


Figure 1. *Top panel:* shell radius (increasing curves) and velocity as a function of time for three SN energies (*solid line:* $E_{SN} = 10^{53}$ erg; *dotted line:* $E_{SN} = 10^{52}$ erg; *dashed line:* $E_{SN} = 10^{51}$ erg). The ISM density is $n_0 = 10^2 \text{ cm}^{-3}$. *Bottom panel:* instability growth rate evolution for the three SN energies. The curves are plotted until the shock decays into a pressure wave.

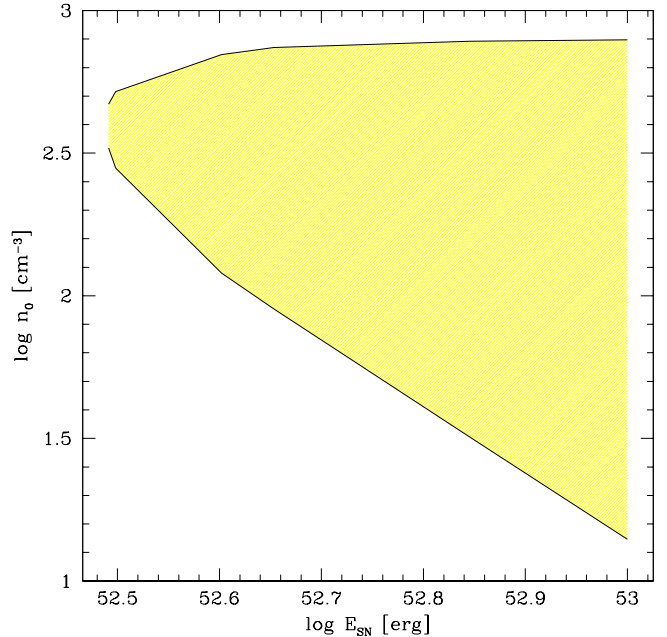


Figure 2. Region of the parameter space ($E_{SN} - n_0$) where both the conditions $\omega > 0$ and $v_{sh} > c_{s,0}$ are verified.

medium, n_0 , and of the density of the thin shell, ρ_{sh} (proportional to the shell swept up mass, and thus function of R_{sh}). The growth time of the unstable fragments is $\sim \omega^{-1}$.

In all unstable cases, the age of the shell is larger than the cooling time and the thin shell approximation is valid ($\Delta R_{sh}/R_{sh} < 10^{-3}$).

The shell becomes unstable after 0.7-7 Myr from the explosion, depending on the SN energy and on the initial density of the medium; the most rapidly growing mode corresponds to a fragment radius of 7-51 pc (the upper limits refer to the lowest density). The corresponding fragment mass is $10^5 - 10^6 M_\odot$, with density, n_{sh} , in the range $8 \times 10^3 - 10^9 \text{ cm}^{-3}$. Large values of the gravitational-to-pressure force ratio ($f \gtrsim 400$) are found in all unstable cases. This is because high shell velocities stretch the perturbations, stabilizing the shell (see Eq. 7) and so the instability conditions are satisfied only when the fragments have collected a sufficiently large mass, yielding large values of f .

NU01 (see their Fig. 6) have shown that primordial filaments fragment into dense clumps whose masses depend on n_{sh} and f . For a quasi-equilibrium clump (i.e. $f \gtrsim 1$), fragmentation proceeds until the fragment is close to the Bonnor-Ebert mass value corresponding to the initial density of the clump* (Palla 2002, Mackey *et al.* 2003). If f is increased to 3, a bifurcation takes place at $n_{sh} \sim 10^5 \text{ cm}^{-3}$. For models with $n_{sh} \gtrsim 10^5 \text{ cm}^{-3}$ the minimum fragment mass is 1-2 M_\odot , while for $n_{sh} \lesssim 10^5 \text{ cm}^{-3}$ it is larger than $\sim 100 M_\odot$. Further increase of f causes the low mass regime to extend down to $n_{sh} \sim 10^4 \text{ cm}^{-3}$. NU01 and NU02 stop their simulations at $f = 5-6$, but large values of f , as those found in fragments originating in the expanding SN $_{\gamma\gamma}$ shell, are likely to induce strong fragmentation also at lower initial densities. The fragmentation proceeds down to smaller subclumps searching for an equilibrium between gravitational and pressure forces (thus decreasing f); at the same time the density of the subclumps tends to increase. For f values greater than 400, this equilibrium cannot be reached before the subclump becomes optically thick to H₂ lines. At this stage, the initial clump has already fragmented into protostellar cores with typical masses $\sim 10^{-2} M_\odot$. Although the exact value of the resulting stellar mass depends on the details of subsequent gas accretion and, possibly, on the merging of protostellar cores, it is unlikely that these are so efficient to form a massive star. In fact, the relaxation time corresponding to the ensemble of $m \sim 10^{-2} M_\odot$ protostellar cores resulting from the fragmentation of a $M_f = 10^5 M_\odot$ clump is ~ 36 Gyr.

5 MIXING EFFICIENCY AND METALLICITY OF THE FRAGMENTS

In order to derive the mean metallicity of the thin shell (and of the fragments), one should be able to follow the mixing of SN ejecta with the shell gas. The standard hydrodynamical response to a sudden release of energy implies that the

* This is strictly true only for $n_{sh} \geq n_{cr} = 10^4 \text{ cm}^{-3}$ where n_{cr} is the critical density which marks the transition from NLTE to LTE regime for H₂ cooling (see discussion in Schneider *et al.* 2002).

two gases (the swept up matter and the ejecta), after crossing their respective shocks find themselves well separated by a contact discontinuity. However, many mechanisms (e.g. cloud crushing, thermal evaporation, hydrodynamical instabilities, effects caused by explosion inside wind-driven shells and by fragmented ejecta) can disrupt the contact discontinuity leading to a mixing of the heavy elements into the swept-up matter in the thin shell (Tenorio-Tagle 1996). A precise description of such physical processes is extremely difficult as it requires ultra-high resolution simulations (de Avillez & Mac Low 2002; Kifonidis *et al.* 2003).

The mean metallicity of the shell (or fragment) is

$$Z_f = f_{mix} \frac{M_{ej}}{M_{sh}} \quad (12)$$

where f_{mix} is the (unknown) mixing factor of ejected matter in the thin shell and M_{ej} is the ejected mass in heavy elements. For SN $_{\gamma\gamma}$, $M_{ej} \simeq 0.4M_\star$ (Heger & Woosley 2002). Even requiring that mixing is very efficient (i.e. $f_{mix} = 1$), we always find that the mean metallicity of the fragments is $10^{-3.5} Z_\odot < Z < 10^{-2.6} Z_\odot$ (the most metal poor fragment being produced by a 10^{53} erg SN exploding in a medium of mean density $n_0 = 14 \text{ cm}^{-3}$). In more realistic cases, however, mixing is likely to be much more inefficient ($f_{mix} \ll 1$), so the above value, $10^{-2.6} Z_\odot$ is a strict upper limit. At face value, if the most iron poor star observed in our Galaxy ([Fe/H] = -5.3, Christlieb *et al.* 2002) formed through this mechanism, it would imply that $f_{mix} \sim 0.03$. Note that in principle zero-metallicity low-mass stars can form via the proposed mechanism if $f_{mix} = 0$.

6 DISCUSSION

We have shown that the explosion of the first pair-instability SNe with $E_{SN} \gtrsim 3 \times 10^{52}$ erg is able to trigger further star formation if these explode in a medium with mean density $n_0 \sim 14 - 790 \text{ cm}^{-3}$. For higher values of n_0 the external pressure efficiently decelerates the shell, which therefore becomes subsonic before the instability sets in. Shells produced by normal or subluminous SNe do not fragment. Fragmenting shells become gravitationally unstable 0.7-7 Myr after the explosion, depending on the explosion energy and density of the unperturbed medium. We have identified the fastest growing mode in the unstable shells and derived the mass, density and gravitational-to-pressure force ratio, f , of the corresponding fragments. Their typical mass is in the range $10^5 - 10^6 M_\odot$, with a corresponding density in the range $8 \times 10^3 - 10^9 \text{ cm}^{-3}$. In all cases, we find very large values of the gravitational-to-pressure force ratio ($f \gtrsim 400$), indicating that the formation of low-mass, long-living stars is the most likely outcome. The mean metallicity of these stars depends on the mixing history of the shell which is largely unknown, as discussed in the previous Section. Depending on the efficiency of this process and on the combined properties of the explosion energy and ambient density, the metallicity of this second generation, low-mass stars can be anywhere in the range $0 \leq Z \leq 10^{-2.6} Z_\odot$.

The mechanism here proposed is thus able to produce long-living, low-mass extremely metal-poor (or even metal-free, if $f_{mix} = 0$) stars that can be found in the Milky Way halo. These stars can populate the low-mass peak of the

bimodal IMF proposed by NU01 and NU02 or can be the typical members of the so-called II.5 population (Mackey *et al.* 2003). The formation of these second generation stars requires the presence of a first generation of massive stars exploding as pair-instability SNe.

So far, only one extremely iron-poor star with $[\text{Fe}/\text{H}] < -5$ has been identified (HE0107-5240, Christlieb *et al.* 2002). If this result were to be confirmed by the analysis of the complete volume sampled by the Hamburg/ESO survey, several implications for the self-propagating star formation mode can be drawn: the observed lack of $[\text{Fe}/\text{H}] < -5$ halo stars would imply that mixing of metals in the unstable shell must occur with moderately high efficiencies ($f_{\text{mix}} \gtrsim 10\%$). Alternatively, the mechanism here proposed might not lead to a large number of observed iron-poor halo stars because: (i) the typical mass of this second-generation stars is $\gtrsim 1-2M_{\odot}$ so that their lifetimes are not long enough to be observable as main sequence stars in our Galaxy halo; (ii) pair-unstable SNe with explosion energies $> 3 \times 10^{52}$ erg are rare because the IMF of the first stars is shaped so that only a small fraction of zero-metallicity massive stars form in the mass range $190M_{\odot} \lesssim M_{\gamma\gamma} \lesssim 260M_{\odot}$ (this constraint can be drawn because the requested range of ISM densities for shell fragmentation is sufficiently large to be easily satisfied).

Conversely, if more very iron-deficient ($[\text{Fe}/\text{H}] < -5$) stars were to be identified, the statistics and properties of these old stellar relics might lead to important constraints on the dominant processes which enable low-mass star formation in primordial environments. In particular, three viable mechanisms have been proposed for the origin of HE0107-5240 (Christlieb *et al.* 2002). Their main difference relies in the interpretation of the observed surface abundance of C and N (and possibly O; Christlieb, private communication). In particular, if one assumes that the observed Fe *is not* a good indicator of the metallicity of the gas cloud out of which the star formed and that C and N were already present in the star forming gas (C, N pre-formation scenario), then HE0107-5240 formed with an initial metallicity of $Z \sim 10^{-2}Z_{\odot}$. Indeed, Umeda & Nomoto (2003) have shown that the abundance pattern of HE0107-5240 is in good agreement with nucleosynthetic yields of a faint SN explosion of a $\sim 25M_{\odot}$ zero-metallicity star releasing a kinetic energy of 0.3×10^{51} erg. If so, due to the small explosion energy, self-propagating star formation could not have occurred and the star must have formed on a longer timescale from the gas enriched by the SN. Alternatively, if one assumes that the observed Fe *is* a good indicator of the parent cloud metallicity and that C and N were synthesized in the stellar interior (C, N post-formation scenario)[†], then HE0107-5240 formed with an initial metallicity of $Z \sim 10^{-5.1}Z_{\odot}$. Indeed, the observed abundance pattern for elements heavier than Mg (that cannot be formed in the interior of a $0.8M_{\odot}$ star such as HE0107-5240 and thus retain memory of the nucleosynthesis yields of the pre-enriching star) are well reproduced

by the predicted yields of a $200M_{\odot}$ pair-unstable SN. In this case, HE0107-5240 could have formed on a short timescale through the self-propagating star formation mechanism or, on a longer timescale, from the gas enriched by the SN if 20% of the metals were depleted onto dust grains (Schneider *et al.* 2003).

ACKNOWLEDGEMENTS

We thank F. Nakamura & M. Umemura for enlightening discussions.

REFERENCES

- Abel T., Bryan G. L., Norman M. L. 2000, ApJ, 540, 39
 de Avillez M. A. & Mac Low M.-M. 2002, ApJ, 581, 1047
 Bromm V., Coppi P. S., Larson R. B. 1999, ApJ, 527, L5
 Bromm V., Ferrara A., Coppi P. S., Larson R. B. 2001, MNRAS, 328, 969
 Bromm V., Coppi P. S., Larson R. B. 2002, ApJ, 564, 23
 Christlieb N., Wisotzki L., Reimers D., Homeier D., Koester D., Heber U. 2001, A&A, 366, 898
 Christlieb N. *et al.* 2002, Nature, 419, 904
 Elmegreen B. G. 1994, ApJ, 427, 384
 Ferrara A. 1998, ApJ, 499, L17
 Heger A. & Woosley S. E. 2002, ApJ, 567, 532
 Kifonidis K., Plewa T., Janka H.-Th., Mueller E. 2003, submitted to A&A, astro-ph/0302239
 Madau P., Ferrara A. & Rees M. J. 2001, ApJ, 555, 92
 Magliocchetti M., Salvaterra R. & Ferrara A. 2003, submitted to MNRAS
 Mackey J., Bromm V. & Hernquist L. 2003, ApJ, 586, 1
 Nakamura F. & Umemura M. 2001, ApJ, 548, 19 (NU01)
 Nakamura F. & Umemura M. 2002, ApJ, 569, 549 (NU02)
 Omukai K. & Inutsuka S. 2002, MNRAS, 332, 59
 Omukai K. & Palla F. 2003, submitted to ApJ, astro-ph/0302345
 Ostriker J. P. & McKee C. F. 1988, Rev. Mod. Phys., 60, 1
 Palla F. 2002, in Physics of Star Formation in Galaxies, ed. A. Maeder & G. Maynet (Berlin: Springer), 16
 Salvaterra R. & Ferrara A. 2003, MNRAS, 339, 973
 Schlattl H., Cassini S., Salaris M., Weiss A. 2001, ApJ, 559, 1082
 Schlattl H., Salaris M., Cassini S., Weiss A. 2002, A&A, 395, 77
 Schneider R., Ferrara A., Natarajan P., Omukai K. 2002, ApJ, 571, 30
 Schneider R., Ferrara A., Salvaterra R., Omukai K., Bromm V. 2003, to be published on Nature
 Sedov, 1959, Similarity and Dimensional Methods in Mechanics, Academy Press, New York
 Seiss, L., Livio, M. & Lattanzio, J. 2002, ApJ, 570, 329
 Shigeyama T. & Tsujimoto T. 1998, ApJ, 507, L135
 Tenorio-Tagle G. 1996, AJ, 111, 1641
 Umeda H. & Nomoto K. 2003, to be published on Nature, astro-ph/0301315

[†] These “post-formation” scenarios require a sensible explanation for the large observed C and N abundances. So far, it is still unclear whether efficient mixing during the He-flash can fully account for the observed abundances or if it had enough time to operate in HE0107-5240 (Schlattl *et al.* 2001, 2002; Siess *et al.* 2002).